Editor, Ocean Science
Email: editorial@copernicus.org

December 4, 2018

Dear Editor:

Thank you for your letter dated September 10 and 16 regarding our manuscript entitled "Could the mesoscale eddies be reproduced and predicted in the northern south China sea: case studies" (No: os-2018-74), which was submitted to Ocean Science for consideration of publication. We have read reviewers' comments carefully. Following your suggestions, we have gone through the manuscript and made the following changes in the manuscript.

The line-by-line replies for reviewers' comments are shown in the attachments. The original comments are quoted in Times New Roman (Bold) and our responses are in Times New Roman.

Once again, thank you and reviewers for the time and energy spending on reading our manuscript and providing constructive comments and suggestions, which are very valuable in improving the quality of our manuscript.

Enclosed, please find our updated manuscript and reply to the reviewers' comments.

We hope this version of our manuscript can meet the standard of publication in this journal, and we look forward to receiving further instruction related to this submission.

Sincerely yours

Dazhi Xu

Responses to Reviewer 1

General comment:

The related studies about the mesoscale eddies in the SCS have amount of achievements, especially owing to the altimeter data widely applied, for understanding the dynamic and the interactions with the environmental current circulations on large scale. The article of "Could the mesoscale eddies be reproduced and predicted in the northern south China sea: case studies" would like focus on two anticyclonic eddies in the northern SCS (NSCS). By helps of a HYCOM-EnOI assimilation system, they found the key of the predictable issues about the eddy generation, evolution and propagation paths can be done well only when the eddy amplitude is larger than 8 cm. Clearly, this topic is interesting for deep understanding the real factors to limit the eddy's forecast performance. The used methods, the related experiments, the main conclusions in this study are creditable. But there are obvious some errors in text and figures/tables, this version needs to be more clear to state the findings and the concerned writings, although don't need to add more experiments.

The main comments and some found errors are listed as follow:

Ans: We greatly appreciate reviewer for the time and energy spending on reading our manuscript and providing constructive comments and suggestions. We totally agree with the reviewer and we made every effort to clarify our results and improve the manuscript. The revised version reflects these changes. The detailed comments have been replied one by one below. Once again, thank you very much for your significant comments and suggestions, which are valuable in improving the quality of our manuscript.

1) Under the current introduction, the reasons why to choose the two eddies in the north SCS are not clear enough. It means the necessity and the representative still need to be highlight. For example, complement the more details about these two eddies: the lifetime (Section 3.1); all the related references; methods and main points in Wang et al. (2008) and then relate to the aims in this study.

Ans: Thank you for these comments. The introduction has been revised, the lifetime, evolution and propagation of these two eddies has been described, farther, the related reference is also been added in the revised versions. (P4 line 61-76).

2) The eddy amplitude of 8 cm is a main finding in this study. For my opinion, it should have a relation with the SLA error in this system. Before the comparison of the eddy paths under different conditions, it is important to evaluate your simulated SLA (like in As_exp) to know how about the uncertainty. So one paragraph should be added.

Ans: Thank you. The paragraph which describe the evaluation of the uncertainty of the CSCASS has been added in the revised versions. (P12, line 227-233).

3) It is important to clearly define how to objectively evaluate the eddy reproduction is well.

In this study, the compared result is referred to the buoy trajectory and the detected by altimetry. Clearly, the related formula as possible can relate to these two elements. It will be helpful to simple and conclude in Table 2 and 3. For instance, P6 L230 "From Fig. 4 and Table 2, we can see that the generation and movement of AE1 can be well reproduced by the CSCASS . . ." add the related error statement and then objectively to know reproduced well or not.

Ans: Thank you for your constructive advice. In the revised version, we used a dimensionless index called advective nonlinearity parameter (ANP, Chelton et al., 2011, Li et al., 2014; 2015; 2016; Wang et al., 2015), which expressed as the maximum rotational speed U divided by the translation speed c of the eddy, that is U/c (P12, line 234-237). As Fig.5 shows, if the U/c > 2 the CSCASS can well reproduce AE2 (P28).

4) P 1 L 51: ". . . high resolution satellite images or numerical model simulations (Yang et al., 2000), . . ." needs to add more reference about the recent key findings about mesoscale eddy both from satellite and modelling like as following:

Fu, L.-L., D.B. Chelton, P.-Y. Le Traon, and R. Morrow. 2010. Eddy dynamics from satellite altimetry. Oceanography 23(4):14–25, https://doi.org/10.5670/oceanog.2010.02.

Morrow, R. and Le Traon, P.-Y. Recent advances in observing mesoscale ocean dynamics with satellite altimetry. Adv. Spa. Res. 50, 1062–1076 (2012).

Frenger, I., Gruber, N., Knutti, R. & Münnich, M. Imprint of southern ocean eddies on winds, clouds and rainfall. Nat. Geosci 6, 608–612 (2013).

Ans: Thank you. The references have been added in the revised versions. (P3, line 40-41).

5) L 52: ". . . the operational forecasts of the mesoscale eddy still poses a big challenge because of its complicated dynamical mechanisms and high nonlinearity (Yuan and Wang, 1986; Li et al., 1998)." These references are not suitable because they are not related with ocean operational forecast and were published more than 20 years out of representing the recent knowledge.

Some references are recommended as follow: De Vos, M., Backeberg, B. and Counillon, F.: Using an eddy-tracking algorithm to understand the impact of assimilating altimetry data on the eddy characteristics of the Agulhas system. Ocean Dyn., https://doi.org/10.1007/s10236-018-1174-4, 2018.

Robert H. Woodham, Oscar Alves, Gary B. Brassington, Robin Robertson & Andrew Kiss (2015) Evaluation of ocean forecast performance for Royal Australian Navy exercise areas in the Tasman Sea, Journal of Operational Oceanography, 8:2, 147-161, DOI: 10.1080/1755876X.2015.1087187

Treguier Anne-Marie, Chassignet Eric P., Le Boyer Arnaud, Pinardi Nadia (2017). Modeling and forecasting the "weather of the ocean" at the mesoscale. J. Marine Research, 75(3), 301-329. http://doi.org/10.1357/002224017821836842.

Ans: Thank you. The references have been added in the revised versions. (P3, line 43)

6) P3 L87: ". . . thus is essential for the prediction of mesoscale eddies (e.g., Xiao et al. 2007; Xie et al., 2011; Xu et al., 2012; Xie et al., 2018)". The concerned assimilation works done in the NSCS needs be commented, and then to be pointed the disadvantages to relate the aims in this study.

Xiao, X., Wang, D., Yan, C., and Xu, J.: The assimilation experiment in the southwestern South China Sea in summer 2000, Chinese Sci. Bull., 51, 31–37, 2007.

Xie, J., Bertino, L., Cardellach, E., Semmling, M., and Wickert, J.: An OSSE evaluation of the GNSS-R altimetery data for the GEROS-ISS mission as a complement to the existing observational networks, Remote Sens. Environ., 209, 152-165, doi:10.1016/j.rse.2018.02.053, 2018.

Xie, J., Counillon, F., Zhu, J., and Bertino, L.: An eddy resolving tidal-driven model of the South China Sea assimilating along-track SLA data using the EnOI, Ocean Sci., 7, 609–627, doi:10.5194/os-7-609-2011, 2011.

Ans: Thank you. The references have been added in the revised versions. (P5, line 91)

7) P5 L131: Are there some cases using this detection scheme in the SCS? Yes, give the reference, otherwise provide a simple snapshot to show its ability.

Ans: Yes, Cheng et al., (2005) used this detection scheme to study the seasonal and interannual variabilities of mesoscale eddies in South China Sea. (P7, line 125)

8) Table 1 lists the designed experiment time. For instance (my personal point), the experiments designed by the eddy strength should be highlighted using one figure to replace the table. On this figure, the eddy strengths of AE1 and AE2 are curved as a function of the date, and the experimental date at beginning also are marked on by vertical lines.

Ans: Thank you. According to your advice, we use Fig.4 to replace table 1. (P28, Fig.4)

9) Table 2: The dates of the first weeks need to be stated. What the differences between "Amplitude" and "Intensity"? As the statement of P4 L127 "the intensity of the mesoscale eddy must be greater than 2 cm;", how the observed amplitudes of AE1/AE2 less than 2 cm? Are they the error or others? And to compare the amplitudes in the first and the second weeks, can comment the big gap?

Ans: Thank you. The dates of the first weeks have been added to table 2 (P31, table1); In the original version, the intensity is the difference between the extremum and the outermost closure of SLA; the amplitude is the difference between the extremum and 0 of SLA. In the revised version, the amplitude is the difference between the extremum and the outermost closure of SLA, and do not use the intensity. The observed amplitudes of AE1/AE2 less than 2 cm are errors and corrected in the revised version (P31, table1).

10) Use the same color in the panel f of Figure 9-11 as the other panels of Fig. 6-8: the blue (red) is forecast (observation), and using full or empty mark to distinguish AE1 and AE2.

Ans: Thank you. The related figures have been revised in the revised versions (P34, Fig.11; P35, Fig.12-13).

11) There are interested finding in Figure 12: at the first stage of AE1 and AE2 the distance error looks decreasing; at end stages the distance error increasing with time. Can you explain the former?

Ans: Thank you! As our results show, at the first stage of AE1 and AE2, they are in strong intensity stage or become more and more strong. The CSCASS, after assimilated SLA and SST, can well reproduce these eddies. But at the end stages, the signals of eddy become weak, so the CSCASS can not catch even assimilated the SLA and SST.

12) In Figure12, add another referenced eddy distance line from As_exp. It will be interesting to compare these two lines to show the predictability if without data assimilation.

Ans: Thank you. The eddy distance line from As_exp has been added to Fig.12 in the revised versions. (P36, Fig.14)

13) Recommend to replace the title by "Could the two anticyclonic eddies during winter 2003/2004 be reproduced and predicted in the northern south China sea?"

Ans: Thank you. The title has been revised in the revised versions. (P1, line 1-2)

Technic comments:

Figure 3 is too ambiguous.

Ans: Thank you. This figure has been changed in the revised versions. (P27, Fig.3)

P1, L62: "... (Fig. 1). Forced . . .";

Ans: Thank you. The word 'Forcing' has been changed to 'Forced' in the revised versions. (P3, line 50)

the intensity of the mesoscale eddy must be greater than 2 cm;

Ans: Thank you. You are right, the intensity of the mesoscale eddy is greater than 2 cm. There is a technical error in the original version, which leads to the intensity of the mesoscale eddy less than 2 cm. This error has been corrected in the revised versions. (P31, table 1)

P5: The paragraph introduces the ocean model should be shorten like deleting the lines of 140-150.

Ans: Thank you. The sentences have been deleted in the revised versions. (P8, line 141-150)

P7 L 170: ". . . as a surface forcing from Legates and Willmott (1990)." Legates, D.R., Willmott, C.J., 1990: Mean seasonal and spatial variability in gauge-corrected, global precipitation. Int. J. Climatology, 10, 111-127.

Ans: Thank you. The reference has been corrected in the revised versions. (P22, line 451-452)

P7, L172: missing the reference of "Han (1984)".

Ans: Thank you. The reference has been added in the revised versions. (P22, line 438-439)

P7, L 183: EnKF as the first place should give the detailed name.

Ans: Thank you. The detailed name of EnKF has been added in the revised versions. (P10, line 182)

P9, Section 3.1: The AE2 lifetime was not clearly stated so the first (last) identified date needs be mentioned.

Ans: Thank you. The first (last) identified date of AE2 has been added in the revised versions. (P4, line 69, line 73)

Table 3: ". . . distance of eddy centers between the observation SLA's . . ." are missing on the content. So double cheek the consistence in caption.

Ans: Thank you. The distance of eddy centers for forecast experiments have been added in the revised versions. (P32, table 2)

Figure 12: The cyan line is hard to see so change it to be black. The histogram should use the rectangle to present well other than circle and triangle. L631:"The red and green histograms indicated the AE1 amplitudes from observation and prediction respectively."

Ans: Thank you. The sentence has been corrected; The circle and triangle have been replaced by the rectangle in the new figure 12 (P36, Fig. 14). Due to the black line has been used to denote AE2, we still use the cyan line denote to AE1 in the revised versions.

The wrong order of the references is clear like: P18 L 414 Bleck et al. (2002); P18 L421 Counillon and Bertino (2009); P18 L433 Hamilton et al. (1999); P19 L444 Kara et al. (2002); P20 L475 Rio et al. (2014); P20 L487 Woodruff et al. (1987)

Ans: Thank you. The order of the references has been corrected in the revised versions. (P21-25, line 410-533)

Responses to Reviewer 2

General comments:

The motion and transport of mesoscale eddies have been intensively studied with the altimeter data. In contrast, the simulations are relatively very few, although they are more useful for prediction and applications. As the simulations in this paper are quite well, I have a few minor comments on results. My major concerns are how to improve the writing skill of the paper to make it more comprehensible and valuable for readers. In final, the result is interesting and valuable, but some minor revisions are required before publication.

Ans: Thank you very much for your supports and valuable comments. We totally agree with the reviewer and we made every effort to clarify our results and improve the manuscript. The revised version reflects these changes. The detailed comments have been replied one by one below. Once again, thank you very much for your significant comments and suggestions, which are valuable in improving the quality of our manuscript.

1. In this paper, both amplitude and intensity are used. In general, eddy amplitude was common used in previous studies (e.g., Chelton et al., 2011). I suggest authors use amplitude other than intensity in the paper

Ans: We totally agree with your comments. The intensity has been removed or changed to amplitude in the revised versions. (P7, line 129; P13, line 258; P14, line 288; P15, line 292; P16, line 317; P18, line 373)

2. The motivation of study may be stressed in a more comprehensive way for board readers, if the authors include the previous knowledge on evolution and propagation of oceanic eddies from altimeter data. The motion of mesoscale eddies would be a straight line, if eddies freely propagate in open ocean. However, most of eddies may have interaction with topography (costal and islands), strong currents (e.g., western boundary current), eddies during their lifetime. The motion of eddy will be modified and even split when approaching an island (Yang et al., 2017). It is also recognized that western boundary is graveyard of eddies (Zhai et al., 2010). The dynamical processes such as splitting and/or merging of eddies can also make termination and/or genesis of eddies in open ocean (Li et al., 2016). Thus the dynamical processes make that the prediction of eddy motion is a challenge for ocean simulation.

Ans: We greatly appreciate your support and constructive comments on our work. We agree with your comments. Thank you for the supportive and constructive comments on our manuscript.

3. The result is useful that generation, evolution and propagation paths of AE1 and AE2 can be well reproduced and forecasted when their amplitude >8 cm. I have two comments on this point. Firstly, authors should clearly point out what "their amplitude" means, observed one or simulated one. Secondly, the values in tables should be clearly consist with this result.

Ans: Thank you. The means of "their amplitude" has been clearly point out, it is the observed amplitude (P2, line 21); There is a technical error in the original version, which leads to the values in tables not consist with the result, the values in the table (P31, table 1) have been corrected in the revised versions.

4. Moreover, amplitude is good criterion, a dimensionless one might be better, which makes the result more valuable. This could be achieved if the authors may go one step further. As we know that mesoscale eddies are nonlinear compare with linear Rossby waves (Chelton et al., 2011), they are quite different, e.g., for propagation speed. It is hypothesized that the advective nonlinearity parameter might be presumably important, and authors may use it as an additional criterion. The advective nonlinearity parameter is defined as the nondimensional ratio U/c, where U is the maximum rotational speed and c is the translation speed of the eddy. A value of U/c> 1 implies theoretically that there is trapped fluid within the eddy interior that is advected with the eddy as the eddy translates, which is a fundamental distinction between linear waves and nonlinear eddies. The authors can check their results: what U/c exactly is in their simulations.

Ans: Thank you for your comments. The advective nonlinearity parameter U/c has been calculated, the results have been shown in Fig.5 (P28) in the revised versions.

Others

Table 3, intensity –> amplitude

Ans: Thank you. The word "intensity" has been changed to "amplitude" in the revised versions. (P32, table 2)

The labels AE1 and AE2 in Figure 1 are coved by symbols. Please shift them away from the symbols, and similar change for Figures 6, 9-11.

Ans: Thank you. The related figures have been corrected in the revised versions. (P26, Fig.1; P33-35, Fig.8-13)

Line 576-579, the order of parameters in table caption are different from that in table. Please modify reorder the parameters.

Ans: Thank you. The table has been corrected in the revised versions. (P32, table 2)

Could the two anticyclonic eddies during winter 2003/2004 be reproduced and predicted in the northern south China sea?~~Could the mesoscale eddies be reproduced and predicted in the northern south China sea: case studies~~

Dazhi Xu [1,3], Wei Zhuang[4], Youfang Yan [2*]

[1]South China Sea Marine Prediction Center, State Oceanic Administration, Guangzhou, China

[2]South China Sea Institute of Oceanology, Chinese Academic of Science, Guangzhou, China

[3]Nansen Environmental and Remote Sensing Center, Bergen, Norway

[4]State Key Laboratory of Marine Environmental Science & College of Ocean and Earth Sciences, Xiamen University, Xiamen 361102, China

带格式的：编号方式：连续

带格式的：编号方式：连续

Abstract

Great progress has been made in understanding the mesoscale eddies and their role on the large-scale structure and circulation of the oceans. However, many questions still remain to be resolved, especially with regard to the reproductivity and predictability of mesoscale eddies. In this study, the reproductivity and predictability of mesoscale eddies in the Northern SCS (NSCS), a region with strong eddy activity, are investigated with a focus on two typical anticyclonic eddies (AE1 and AE2) based on a HYCOM-EnOI Assimilated System. The comparisons of assimilated results and observations suggest that generation, evolution and propagation paths of AE1 and AE2 can be well reproduced and forecasted when the~~ir~~ observed amplitude >8 cm (or the advective nonlinearity parameter U/c greater than 2), although their forcing mechanisms are quite different. However, when their amplitudes~~intensities~~ are less than 8 cm, the generation and decay of these two mesoscale eddies cannot be well reproduced and predicted by the system. This result suggests, in addition to dynamical mechanisms, the spatial resolution of assimilation observation data and numerical models must be taken into account in reproducing and predicting mesoscale eddies in the NSCS.

Keywords: HYCOM; EnOI; Northern South China Sea; Mesoscale eddy; Predictability

1. Introduction

Equivalent to the synoptic variability of the atmosphere, the ocean mesoscale eddies is often described as the "weather" of the ocean, with typical spatial scales of ~100 km and time scales of a month (Wang et al., 1996; Liu et al., 2001; Chelton et al., 2011). The mesoscale eddy is characterized by temperature and salinity anomalies with associated flow anomalies, exhibiting different properties to their surroundings, thus allowing them to control the strength of mean currents and to transport heat, salt, and biogeochemical tracers around the ocean. Although today, the beauty and complexity of these mesoscale features can be seen by viewing high resolution satellite images or numerical model simulations (Yang et al., 2000; Fu et al., 2010; Morrow and Le Traon, 2012; Frenger et al., 2013), the operational forecasts of the mesoscale eddy still pose a big challenge because of its complicated dynamical mechanisms and high nonlinearity (Woodham, et al. 2015; Treguier, et al. 2017; Vos et al. 2018). A recent example is the explosion of the Deepwater Horizon drilling platform in the northern Gulf of Mexico in 2010 where an accurate prediction of the position and propagation of the Loop Current eddy was essential in determining if the spilled oil would be advected to the Atlantic Ocean or still remain within the Gulf (Treguier et al., 2017).

Similar to Gulf of Mexico, the South China Sea (SCS) is also a large semi-closed marginal sea in the northwest Pacific, connecting to the western Pacific through the Luzon Strait (Fig. 1). ~~Forcing~~ Forced by seasonal monsoon winds, the intrusion of Kuroshio Current (KC), the Rossby waves and the complex topography, the SCS, especially the Northern SCS (NSCS) exhibits a significantly high mesoscale eddy

带格式的

activity (Fig. 2). Many studies have tried to investigate the mesoscale eddy in the NSCS (Wang et al., 2003; Jia et al., 2005; Wang et al., 2008). Based on the potential vorticity conservation equation and in-situ survey data, Yuan and Wang (1986) pointed out that the bottom topography forcing might be the primary factor for the formation of anticyclonic eddies in the northeast of Dongsha Islands (DIs). Using survey CTD data in September 1994, Li et al. (1998) recorded the evidence of anticyclonic eddies in the NSCS and suggested these anticyclonic eddies are probably shed from the KC. Investigations by Wu et al. (2007) showed that westward propagating eddies in the NSCS originate near the Luzon Strait rather than coming from the western Pacific. Based on the altimeter, the trajectory of drift and the hydrological observations data, Wang et al. (2008) studied the evolution and migration of two anticyclonic eddies in the NSCS during winter of 2003/2004. As they described, the AE1 generated by interaction of the unstable rotating fluid with the sharp topography of DIs firstly appeared near DIs on the 10th of December 2003 (see Fig. 3). Then it began to move southwestward with its amplitude decreasing gradually. During the movement of AE1, another anticyclonic eddy (AE2) was shed and developed from the loop current of Kuroshio near the Luzon Strait on the 14th of January 2004. The amplitude of AE2 was then increased when it propagated southwestward (Fig. 3d-3f). About five weeks later, AE2 reached its maximum in amplitude and then lasted around three weeks in its mature state. During its decay phase, AE2 moved southwestward quickly with its amplitude decreasing, and finally disappeared at the location of 114°E, 18°N on the 7th of April 2004. In the meanwhile, AE1 continued moving to southwest and eventually

带格式的：上标

带格式的：上标

带格式的：上标

disappeared in the southeastern of Hainan. In addition to physical characteristics, the phytoplankton community at these two eddies have also been studied by Huang et al. (2010). ~~Based on the sea surface height anomaly from satellites, Wang et al. (2008) found a high frequent occurrence of mesoscale eddies in the NSCS, and indicated that the interaction between strong ocean currents and the local topography can generate anticyclonic eddies there.~~ These studies improved our understanding of activities of mesoscale eddy and its possible dynamical mechanisms in the NSCS.

Despite the studies on the activities and its possible dynamical mechanisms of mesoscale eddies in the NSCS have received much attention in past decades, studies on the reproductivity and predictability of mesoscale eddies in the NSCS are still rare. As mentioned above, mesoscale eddies are not only related to complicated dynamical mechanisms but also involve strong nonlinear processes (Oey et al., 2005) thus they are not a deterministic response to atmospheric forcing. The quality of mesoscale eddies forecasting will depend primarily on the quality of the initial conditions. Ocean data assimilation, which combines observations with the numerical model, can provide more realistic initial conditions and thus is essential for the prediction of mesoscale eddies (Xiao et al. 2006; Xie et al. 2011; Xu et al. 2012; Xie et al. 2018). In this study, we assessed the reproduction and predictability of two typical anticyclonic eddies in the NSCS with focus on their generation, evolution and decay processes by a series of numerical experiments based on a Chinese Shelf/Coastal Seas Assimilation System (CSCASS; Li, 2009; Li et al., 2010; Zhu, 2011) along with the observation data from surface drifter trajectory and satellite remote sensing.

2. Datasets and Methodologies

2.1 Datasets

In this study, the altimetric data between 2003-2004, which includes along-track SLA, totally 29 passes (about 9300 points) over the domain of CSCS was selected. Considering the noise of SLA measurement in the shallow seas, data for the shallow areas with depth<400 m was excluded. In order to verify, the merged SLA based on Jason-1, TOPEX/Poseidon, ERS-2 and ENVISAT (Ducet et al., 2000) provided by Archiving, Validation and Interpretation of Satellites Oceanographic data (AVISO) at Centre Localization Satellite (CLS, ftp://ftp.aviso.oceanobs.com/global/nrt/) with 1/4° x 1/4° resolution and weekly average are used. In addition, because the SLA present only the anomalies relative to a time-mean sea level field, thus a new mean dynamic topography (nMDT), which has been corrected using iterative method by Xu et al. (2012) was used to calculate the realistic sea level in this study.

In addition to SLA datasets, the daily OISST from the National Oceanic and Atmospheric Administration's (NOAA) National Climatic Data Center (ftp://eclipse.ncdc.noaa.gov/pub/OI-daily-v2/NetCDF/), which was merged by an optimum interpolation method (Reynolds et al., 2007) based on the Infrared SST collected by the Advanced Very High Resolution Radiometer sensors on the NOAA Polar Orbiting Environmental Satellite and SST from Advanced Microwave Scanning Radiometer for the Earth Observing System are also used. The daily OISST's biases were fixed using in situ data from ships and buoys. The dataset between 2003 and 2004 was used in this study, with a spatial resolution of 1/4°×1/4°. In addition, the surface

drifting buoy data from the World Ocean Circulation Experiment (WOCE, ftp://ftp.aoml.noaa.gov/pub/phod/buoydata/) are also used. A total of 3 drifters designed to drift at the surface within the upper 15 m and tracked by the ARGOS satellite system. Positions of the drifters were smoothed using a Gaussian-filter scale of 24 h to eliminate tidal and inertial currents, and were subsampled at 6-h intervals (Hamilton et al., 1999).

2.2 Method of identify the mesoscale eddies

Similar to the standard of Cheng et al., (2005) and Chelton et al., (2011), we identify the mesoscale eddies in this study is as follows: 1) there must be a closure contour on the merged SLA; 2) there must have one maximum or minimum inside the area of closure contour for anticyclonic or cyclonic eddy; 3) the difference between the extremum and the outermost closure of SLA, that is, the amplitude~~intensity~~ of the mesoscale eddy must be greater than 2 cm; and 4) the spatial scale of the eddy should be 45-500 km. In addition, the amplitude (A) of an eddy is defined here to be the magnitude of the difference between the estimated basal height of the eddy boundary and the extremum value of SSH within the eddy interior: $A=|h_{ext}-h_0|$.

2.3 Ocean model

We here used a three-dimensional hybrid coordinate ocean model (HYCOM; Halliwell et al., 1998; 2000; Bleck, 2002; Halliwell, 2004; Chassignet et al., 2007) to provide a dynamical interpolator of observation data in the assimilation system. HYCOM is a primitive equation general ocean circulation model with vertical coordinates: isopycnic coordinate in the open stratified ocean, the geopotential (or z) coordinate in the weak stratified upper ocean, and the terrain following sigma-

coordinate in shallow coastal regions. ~~The general equations and numerical algorithms of model in terms of three dimensions velocity field $\vec{u}(u,v,w)$, pressure p, in situ density ρ and the conservation of temperature (θ) and salinity (S) are follows:~~

~~$$\frac{\partial}{\partial t_s}\left(\frac{\partial p}{\partial s}\right)+\nabla_s\bullet\left(\vec{V}\frac{\partial p}{\partial s}\right)+\frac{\partial}{\partial s}\left(\frac{\partial s}{\partial t}\frac{\partial p}{\partial s}\right)=0 \quad (1)$$~~

~~$$\frac{\partial \vec{V}}{\partial t_s}+\nabla_s\frac{\vec{V}^2}{2}+(\xi+f)\vec{k}\times\vec{V}+\left(\frac{\partial s}{\partial t}\frac{\partial p}{\partial s}\right)\frac{\partial \vec{V}}{\partial p}+\nabla_s M-p\nabla_s\alpha=-g\frac{\partial \vec{\tau}}{\partial p}+\left(\frac{\partial p}{\partial s}\right)^{-1}\nabla_s\bullet\left(\vartheta\frac{\partial p}{\partial s}\nabla_s\vec{V}\right) \quad (2)$$~~

~~$$\frac{\partial}{\partial t_s}\left(\frac{\partial p}{\partial s}\theta\right)+\nabla_s\bullet\left(\vec{V}\frac{\partial p}{\partial s}\theta\right)+\frac{\partial}{\partial s}\left(\frac{\partial s}{\partial t}\frac{\partial p}{\partial s}\theta\right)=\nabla_s\bullet\left(\vartheta\frac{\partial p}{\partial s}\nabla_s\theta\right)+\hbar_\theta \quad (3)$$~~

~~where p is pressure, s is the vertical coordinate, $\vec{V}=(u,v)$ is the horizontal velocity, $\xi=\partial v/\partial x_s-\partial u/\partial y_s$ is relative vorticity, $M=gz+p\alpha$ is Montgomery function, $\Theta=gz$ is the gravitational potential, f is the Coriolis parameter, $\vec{k}$ is the unit vector in the vertical direction, ϑ is viscidity coefficient, τ is the wind stress.~~

In this study, HYCOM was implemented in the Chinese shelf/coastal seas with a horizontal resolution of 1/12°×1/12°, and in the remaining regions with 1/8°×1/8°, the model domain is from 0°N to 53°N and from 99°E to 143°E, the detail model domain and grid can refer to the inset panel of Fig.1. The vertical water column from the sea surface to the bottom was divided into 22 levels. The K-Profile Parameterization (KPP; Large et al., 1994), which has proved to be an efficient mixing parameterization in many oceanic circulation models, was used here. The bathymetry data of the model domain were taken from the 2-Minute Gridded Global Relief Data (ETOPO2).

带格式的：正文

带格式的：段落间距段前：0 磅，段后：0 磅

To adjust the model dynamics and achieve a perpetually repeating seasonal cycle before applying the interannual atmospheric forcing, the model was initialized with climatological temperature and salinity from the World Ocean Atlas 2001 (WOA01; Boyer et al., 2005) and was driven by the Comprehensive Ocean-Atmosphere Data Set (COADS; Woodruff et al., 1987) in the spin-up stage. After integrating ten model years with climatological forcing, the model was forced by the European Center for Medium-Range Weather Forecasts (ECMWF) 6-hourly reanalysis dataset (Uppala et al., 2005) from 1997 to 2003. The wind velocity (10-m) components were converted to stresses using a stability dependent drag coefficient from Kara et al. (2002). Thermal forcing included air temperature, relative humidity and radiation (shortwave and longwave) fluxes. Precipitation was also used as a surface forcing from Legates et al. (1990). Surface latent and sensible heat fluxes were calculated using bulk formulae (Han, 1984). Monthly river runoff was parameterized as a surface precipitation flux in the ECS, the SCS and Luzon Strait (LS) from the river discharge stations of the Global Runoff Data Centre (GRDC) (http://www.bafg.de), and scaled as in Dai et al. (2002). Temperature, salinity and currents at the open boundaries were provided by an India-Pacific domain HYCOM simulation at 1/4°×1/4° spatial resolution (Yan et al., 2007). Surface temperature and salinity were relaxed to climate on a time scale of 100 days. Both two-dimensional barotropic fields such as Sea Surface Height and barotropic velocities, and three-dimensional baroclinic fields such as currents, temperature, salinity and density were stored daily.

2.4 The assimilation scheme

The ensemble optimal interpolation scheme (EnOI; Oke et al., 2002), which is regarded as a simplified implementation of the Ensemble Kalman Filter (EnKF), aims at alleviating the computational burden of the EnKF by using stationary ensembles to propagate the observed information to the model space. The data assimilation schemes can be briefly written as (Oke et al., 2010):

$$\vec{\psi}^{a} = \vec{\psi}^{b} + K(\vec{d} - H\vec{\psi}^{b}) \quad (41)$$

$$K = P^{b}H^{T}[HP^{b}H^{T} + R]^{-1} \quad (52)$$

where $\vec{\psi}$ is the model state vectors including model temperature, layer thickness and velocity; Superscripts a and b denote analysis and background, respectively; $\vec{d}$ is the measurement vector that consists of SST and SLA observations; K is the gain matrix; and H is the measurement operator that transforms the model state to observation space. P is the background error covariance and R is the measurement error covariance. In EnOI, Eq. 5 2 can be expressed as:

$$K = \alpha(\sigma \circ P^{b})H^{T}[\alpha H(\sigma \circ P^{b})H^{T} + R]^{-1} \quad (63)$$

where α is a scalar that can tune the magnitude of the analysis increment; σ is a correlation function for localization; and P^{b} is the background error covariance which can be estimated by

$$P^{b} = A'A'^{T}/(n-1) \quad (74)$$

In Eq. 74, n is the ensemble size, A' is the anomaly of the ensemble matrix, $A = (\psi_1, \psi_2, \cdots, \psi_N) \in \Re^{n\times N}$ ($\psi_i \in \Re^{N}(i = 1, \cdots, n)$ is the ensemble members, N is the dimension of the model state, representing usually the model variability at certain scales by using a long-term model run or spin-up run. More detailed description and

evaluation of the CSCASS in Li et a., (2010) and Xu et al., (2012).

3. Results

~~### 3.1 The observation of two anticyclonic eddies in the NSCS~~

~~In this study, we investigated two representative anticyclonic eddies in the NSCS, one generated in the interior (named AE1) and another shed from the Kuroshio loop (named AE2). The AE1 generated by interaction of the unstable rotating fluid with the sharp topography of DIs (Wang et al., 2008) firstly appeared near DIs on the 10th of December 2003 (see Fig. 3). Then it began to move southwestward with its amplitude decreasing gradually. During the movement of AE1, another anticyclonic eddy (AE2) was shed and developed from the loop current of Kuroshio near the Luzon Strait. The amplitude of AE2 was then increased when it propagated southwestward (Fig. 3d-3f). About five weeks later, AE2 reached its maximum in amplitude and then lasted around three weeks in its mature state. During its decay phase, AE2 moved southwestward quickly with its amplitude decreasing, and finally disappeared at the location of 114°E, 18°N. In the meanwhile, AE1 continued moving to southwest and eventually disappeared in the southeastern of Hainan.~~

带格式的：段落间距段后：7.8 磅

3.~~2~~ 1 The reproduction of these anticyclonic eddies in the NSCS

带格式的：段落间距段前：0 磅

In order to investigate whether the evolution and migration features of these two eddies can be reproduced by the CSCASS or not, we firstly set up an assimilation experiment named As_exp (see ~~Table 1~~Fig. 4, black line) for AE1 and AE2. In this

experiment, the observed SST and SLA are both assimilated into CSCASS at an equal interval of every 3 days. To meet dynamic adjustment, the first assimilation was performed on the 27th of September 2003, two months prior to the generation of AE1.

Base on the As_exp experiment output, we use the observations SLA to evaluate the uncertainty of CSCASS in the research area. In this study, we calculated the weekly mean RMS error (RMSE) of the As_exp /control experiments output and observations for SLA. As the result indicates, the RMSE for the As_exp is between 6 cm to 14 cm, while RMSE for the control is between 10 cm to 18 cm. This result suggested that data assimilation improved effectively the SLA field and had a beneficial impact on model results in this area.

In addition, we also use the Advective Nonlinearity Parameter U/c (ANP, Chelton et al., 2011; Li et al., 2014; 2015; 2016; Wang et al., 2015) as a criterion to estimate the eddy forecast ability of the CSCASS. As fig. 5 shows, when the ANP greater than 2 (that is the amplitude greater than 8 cm) AE2 can be well reproduced by the CSCASS.

Besides, we also use the independent evaluation, Fig.~~ure 4~~6 compared the assimilating results of AE1 with the observations both from the satellite remote sensing and drifter buoys trajectories of number 22517, 22918 and 22610 between December 3rd 2003 and February 18th 2004. From Fig. ~~4~~ 6 and Table ~~2~~1, we can see that the generation and movement of AE1 can be well reproduced by the CSCASS, with the pink curves (assimilation) match well with those of black (satellite observations) and dotted lines ~~–~~(the trajectories of drifter buoys). In addition, the spatial pattern of AE1 can also be well revealed by the CSCASS: the radius of meridional and zonal of AE1

detected by the assimilation are 163 km and 93 km, which are almost equal to that of observations (148 km and 79 km). The migration path of AE1 can also be well reproduced by the CSCASS (see Fig. ~~4~~6, black and pink line) until its amplitude decays to less than 8 cm. In addition to AE1, the generation and evolution of AE2 are also evaluated. As shown Fig. ~~5~~7, the evolution and propagation pathway of AE2 (Fig. ~~5b~~7b-~~5j~~7j), e.g., move northwestward firstly and then southwestward can generally be reproduced by the CSCASS, although its initial location shows a slight southward bias in the simulation (Fig. ~~5a~~7a). Similar to the results of AE1, discrepancies between model and observations become larger again during the decay phase of AE2.

In general, the comparison of assimilation SLA with that of satellite observation and the trajectories of drifter buoys suggested that the generation, development and the propagation of AE1 and AE2 can be reproduced by the CSCASS when their amplitude greater than 8 cm (or the ANP greater than 2). However, when their amplitudes~~intensity~~ are relatively ~~weak~~small, with ~~amplitude~~values less than 8 cm, the features of these two mesoscale eddies are not well reproduced by the CSCASS. This may be related to the value setting of parameter α, the localization length scale, and insufficient spatial resolution of assimilating SSH or the numerical model (Counillon and Bertino, 2009).

3.~~3~~ 2 The predictability of these anticyclonic eddies in the NSCS

Since the generation, development and the propagation of AE1 and AE2 can be well reproduced by the CSCASS when their amplitude>8 cm (or the ANP greater than 2), as mentioned above, in this section we further use the CSCASS to investigate the predictability of these two eddies. According to the generation, evolution and migration

of these two eddies, we designed six forecast experiments, hereafter referred to as Exp1 to Exp6 (see ~~Table 1~~Fig.4) to investigate their predictability. The model's initial state prior to each of the six forecast experiments is constrained by assimilating satellite SLA and SST before. Based on the initial state, each experiment is run forward 30 days with the forcing of 6-hourly wind, surface heat flux, and monthly mean river runoff, etc. The first experiment, named Exp1, is applied on the 29th of November 2003, which tends to study whether the generation of AE1 can be forecasted or not. Exp2 is implemented on the 10th of December 2003 and is used to study whether the development and the migration of AE1 can be forecasted. Exp3 is run based on the initial state on the 31th of December 2003 and used to show whether the generation of AE2 and the continued migration of AE1 can be forecasted. In order to investigate whether the continued evolution of AE1 and AE2 can be forecasted, Exp4 is applied on the 21th of January 2003. Exp5, is setting up to reveal whether the attenuation of AE1 and the evolution of AE2 can be forecasted, while Exp6 which is applied on the 29th of February 2004 was designed to find out whether the disappear of AE1 and AE2 can be forecasted.

The prediction results of Exp1 are shown in Fig. ~~6~~8. In Fig. ~~6~~8a, we can see that the forecast is almost coincident with the satellite observation and the trajectory of drift buoys, indicating that the generated position of AE1 can be well forecasted by the CSCASS. In addition, the initial migration of AE1 can also be forecasted by the CSCASS (see Fig. ~~6~~8a and ~~6~~8f). In order to evaluate the forecasted amplitude of AE1, the ~~intensity,~~ amplitude and the distance of eddy centers between the observation and the forecast are also quantified (Table ~~3~~2: EXP1). From Table ~~3~~2: EXP1, we can see

that the amplitude of forecasting matches well with that of observation, although its amplitude is slightly larger than that of observation. After 4 weeks, the amplitude ~~and intensity~~ of the forecast ~~are~~ is still close to those of the observation, suggesting that the generation of AE1 can be well predicted by the CSCASS.

In order to find out whether the development and movement path of AE1 can be predicted after generation, we continue to carry out Exp2. As shown by the observation (Fig. ~~7~~9), AE1 moves southwestward along the continental shelf with its amplitude decreasing and again increasing after its generation. This observed southwestward movement is also predicted by the CSCASS (see pink closure curve in Fig. ~~7~~9a-~~7~~9d), although a sudden southwestward movement cannot be well predicted (Fig. ~~7~~9f). In addition, the first attenuation and then enhance of AE1 can also been predicted by the CSCASS (see Table ~~3~~2 and Fig. ~~7~~9b). On the whole, the development and movement path of AE1 can be well predicted by CSCASS for the first four weeks after its generation. After that, the errors between observation and prediction increase significantly, and by the fifth week, the distance between the center of the prediction and the observation become larger, which more than 100 km (see Fig. ~~7~~9e).

For further analysis, we carry out Exp3, to look at whether the continue evolution of AE1 and the generation of AE2 can be predicted. This experiment is carried out based on the initial condition of the assimilation on the 31st of December 2003 and the corresponding results are shown in Fig. ~~8~~ 10 and Table ~~3~~2. ~~The development trend of AE1 can be predicted, but with a slightly weak amplitude, a~~As shown by the prediction (Fig. ~~8~~10, Table ~~3~~2), although with a slightly weak amplitude, the CSCASS can

reproduced AE1 after assimilating SLA and SST and predicted its development trend. ~~The observed center elevation of AE1 reduced from 18 cm in the first week to 13 cm in the fifth week. Similar decreasing trend was also found for the forecast but with its amplitude decreasing from 13 cm at the beginning to 10 cm at the end of the forecast period. Although the decreasing trend of AE1 amplitude is quite similar between the observations and forecast, their intensity is slightly different.~~ In addition, the movement path of AE1 cannot be accurately predicted at this period, for instance, the observed AE1 moves directly to southwest (see red solid line and solid circle in Fig. ~~8f~~10f), but the prediction's movement firstly toward northeast, then turns to southwest (see blue solid line and solid circle in Fig. 10~~8~~f). The generation of AE2 cannot be predicted in Exp3, which may be related to the ~~lower~~ smaller amplitude (<8 cm) of AE2 at this period.

The purpose of Exp4 is to look at whether the evolution of AE1 and AE2 can both be reasonably predicted. Since this experiment mainly focuses on the evolution of AE1 and AE2, thus Fig. ~~9~~ 11 shows only the evolution of AE2 from the second week after generation, that is, from the beginning on the 21st of January 2004 to the fifth week. As shown in Fig. ~~9~~11, Table ~~3~~ 2 and Fig. ~~12d~~14d, the trends of amplitude variation of both eddies can be well predicted with the decreasing of AE1 and slowly increasing of AE2. For AE1, the results of the prediction and observation are very close in the first two weeks, with the center of the two almost coincide. The central position of the prediction and observation began to deviate after the third week. For AE2, although the amplitude and movement path are not predicted well at its initial stage, the prediction is slowly

approaching to the observation during third to fifth week, and distance between the center of the prediction and the observation is reduced from 132 km at the beginning to 81 km at the end (see Fig. ~~12d~~ 14d the black solid line).

As mentioned above, the purpose of Exp5 is to investigate whether the decay of AE1 and the continued development of AE2 can be predicted. From Fig. ~~10~~12, Table ~~3~~ 2 and Fig. ~~12e~~14e, we can find that the CSCASS cannot predict the movement path of AE1 well in its decay stage: the distance between the center of the prediction and that of the observation is greater than 188 km, and the moving direction of the two is not consistent (see red lines and dots in Fig. ~~10f~~12f). But the evolution and moving direction of AE2 can be well predicted at this stage. The amplitude of observation and prediction of AE2 are keeping in the consistent trend (Fig. ~~12e~~14e), although the speed of movement of AE2 given by prediction is slower than that of observation (see ~~green~~ blue dashed lines and hollow dots in Fig. ~~10f~~12f).

The aim of Exp6 is to find whether the disappearance of AE1 and AE2 can be both predicted. As described in Fig. ~~11~~13, the disappearance of AE1 cannot be well predicted since the low amplitude (less than 8 cm) of AE1 at this stage. Similarly, the disappearance of AE2 is also less accurately predicted by the CSCASS (Fig. ~~12f~~14f). The amplitude of AE2 from the observation decays continually at this stage, but the amplitude of the predicted almost keeps constant. In addition, there is large deviation of the direction of movement between prediction and observation for AE2 (see the red solid line and dot in Fig. ~~11f~~13f).

4. Conclusions and challenges for forecasting of mesoscale eddy

In this paper, we carry out a series of assimilation and prediction experiments by the CSCASS to assess the productivity and predictability of mesoscale eddies in the NSCS, along with observations of satellite observed SST, SLA and the trajectory data of drift. The comparisons of AE1 and AE2 by the CSCASS, which is assimilated SLA and SST, with that of observations through predicted experiments shows that when the amplitudes of mesoscale eddy are higher than 8 cm, the generation, development, decay and movement of eddies can be well reproduced, but when the amplitude of the mesoscale eddy is lower than 8 cm, the generation and disappear of mesoscale eddy cannot be well reproduced.

The comparisons of AE1 and AE2 through six predicted experiments with those of observations also show that the generation, evolution and movement path of these two eddies with high amplitude (>8 cm or the ANP greater than 2) can be well predicted by the CSCASS, although the generative mechanism of these two eddies is quite different (Wang et al., 2008)[9]. However, when the amplitude of eddies becomes less than 8 cm, the generation position and the movement path cannot be well predicted by the CSCASS.

Our results suggested that for ~~intensity~~ powerful mesoscale eddies, a good initial condition after assimilating observations can help to improve their reproduced and predictable ability. As mentioned above, the mesoscale eddies are related to strong nonlinear processes and are not a deterministic response to atmospheric forcing, thus the quality of mesoscale eddies forecast will depend primarily on the quality of the

带格式的：非上标/ 下标

initial conditions. In addition, the ability of the ocean numerical model to faithfully represent the ocean physics and dynamics is also crucial. Although data assimilation, which combines observations with the numerical model, can provide good initial conditions, it cannot make up the limitations of numerical model in numerical algorithms and in its resolution. For a high-resolution operational oceanography, the latter means that the numerical models need to be improved using more accurate numerical algorithms and resolution especially in the weakly stratified regions or on the continental shelf.

Furthermore, so far most of the information about the ocean variability is obtained remotely from satellites (SSH and SST), the information about the subsurface variability are very rare. Although a substantial source of subsurface data is provided by the vertical profiles (i.e., expendable bathy thermographs, conductivity temperature depth, and Argo floats), the datasets are still not sufficient to determine the state of the ocean. In addition, in order to accurately assimilate the SSH anomalies from satellite altimeter data into the numerical model, it is necessary to know the oceanic mean SSH over the time period of the altimeter observations (Xu et al., 2011; Rio et al., 2014). This is also a big challenge because the earth's geoid is not presented with sufficient spatial resolution when assimilating SSH in an eddy-resolving model. With the advent of the SWOT (Surface Water and Ocean Topography) satellite mission in 2020, it should be possible to better resolve and forecast the mesoscale features in eddy resolving ocean forecasting systems.

Acknowledgements:

This study is supported by the Marine Science and Technology Foundation of South China Sea Branch, State Oceanic Administration (grant 1447), the National Key Research and Development Program of China (2016YFC1401407), the Project of Global Change and Air-Sea interaction under contract No. GASI-03-IPOVAI-04, the National Natural Science Foundation of China (Grant No. 41776037 and 41276027), and the China Scholarship Council (award to Xu Dazhi for 1 year's study abroad at Nansen Environmental and Remote Sensing Center).

带格式的

References:

Bleck R, 2002. An oceanic general circulation model framed in hybrid isopycnic cartesian coordinates. Ocean Modelling, 4(1): 55-88.

Boyer T P, Levitus S, Antonov J I, Locarnini R A, Garcia H E, 2005. Linear trends in salinity for the World Ocean, 1955-1998. Geophysical Research Letters, 32(1): 67-106.

Chassignet E P, Hurlburt H E, Smedstad O M, et al., 2007. The HYCOM (Hybrid Coordinate Ocean Model) data assimilative system. Journal of Marine Systems, 65(1-4):60-83.

Chelton D B, Schlax M G, Samelson R M, 2011. Global observations of nonlinear mesoscale eddies. Progress in Oceanography, 91(2): 167-216.

Cheng X H, Qi Y Q, Wang W Q, 2005. Seasonal and Interannual Variabilities of Mesoscale Eddies in South China Sea. Journal of Tropical Oceanography, 24(4): 51-59.

Counillon F, Bertino L, 2009. Ensemble Optimal Interpolation: multivariate properties in the Gulf of Mexico. Tellus, 61A: 296-308.

Dai A, Trenberth K E, 2002. Estimates of freshwater discharge from continents: latitudinal and seasonal variations. Journal of Hydrometeorology, 3(6): 660-685.

Ducet N, LeTraon P Y, Reverdin G, 2000. Global high-resolution mapping of ocean circulation from TOPEX/Poseidon and ERS-1 and-2. Journal Geophysical Research, 105(C8): 19477-19498.

Frenger I, Gruber N, Knutti R, Münnich M, 2013. Imprint of Southern Ocean eddies on winds, clouds and rainfall. Nature Geoscience, 6, 608-612.

Fu L-L, Chelton D B, Traon P-Y L, Morrow R, 2010. Eddy dynamics from satellite altimetry. Oceanography, 23(4):14-25.

Halliwell J G R, 2004. Evaluation of vertical coordinate and vertical mixing algorithms in the HYbrid-Coordinate Ocean Model (HYCOM). Ocean Modelling, 7(3-4): 285-322.

Halliwell J G R, Bleck R, Chassignet E P, 1998. Atlantic Ocean simulations performed using a new Hybrid Coordinate Ocean Model (HYCOM). EOS, Fall AGU Meeting.

Halliwell J G R, Bleck R, Chassignet E P, Smith L T, 2000. Mixed layer model validation in Atlantic Ocean simulations using the Hybrid Coordinate Ocean Model (HYCOM). EOS,

80, OS304.

Han Y–J, 1984. A numerical world ocean general circulation model: Part II. A baroclinic experiment. Dynamics of Atmospheres and Oceans, 8(2):141-172.

Hamilton P, Fargion G S, Biggs D C, 1999. Loop Current eddy paths in the western Gulf of Mexico. Journal of Physical Oceanography, 29(6): 1180-1207.

Huang B Q, Hua J, Xu H Z, Cao Z R, Wang D X, 2010. Phytoplankton community at warm eddies in the northern South China Sea in winter 2003/2004. Deep-Sea Research II, 57(19-20): 1792-1798.

Jia Y, Liu Q, Liu W, 2005. Primary studies of the mechanism of eddy shedding from the Kuroshio bend in Luzon Strait. Journal of Oceanography, 61(6): 1017-1027.

Kara A B, Rochford P A, Hurlburt H E. 2002. Air-sea flux estimates and the 1997-1998 ENSO event. Boundary-Layer Meteorology, 103(3): 439-458.

Large W G, McWilliams J C, Doney S C, 1994. Oceanic vertical mixing: a review and a model with a nonlocal boundary layer parameterization. Reviews Geophysics, 32(4): 363-403.

Legates D R, Willmott C J, 1990. Mean seasonal and spatial variability in gauge-corrected, global precipitation. International Journal of Climatology. 10(2): 111-127.

Li L, Nowlin W D, Su J L, 1998. Anticyclonic rings from the Kuroshio in the South China Sea. Deep-Sea Research, Part I, 45: 1469-1482.

Li Q Y, Sun L, 2015. Technical Note: Watershed strategy for oceanic mesoscale eddy splitting, Ocean Science, 11(2): 269-273, doi:10.5194/os-11-269-2015.

Li Q Y, Sun L, Lin S-F, 2016. GEM: a dynamic tracking model for mesoscale eddies in the ocean, Ocean Science, 12: 1249-1267, doi:10.5194/os-12-1249-2016.

Li Q Y, Sun L, Liu S-S, Xian T, Yan Y-F, 2014. A new mononuclear eddy identification method with simple splitting strategies. Remote Sensing Letters, 5(1): 65-72. Doi:10.1080/2150704X.2013.872814.

Li X C, 2009. Applying a new localization optimal interpolation assimilation module to assimilate sea surface temperature and sea level anomaly into the Chinese Shelf/Coastal Seas model and carry out hindcasted experiment. Graduate University of the Chinese Academy of Sciences, 92pp.

Li X C, Zhu J, Xiao Y G, Wang R W, 2010. A Model-Based Observation Thinning Scheme for

the Assimilation of High-Resolution SST in the Shelf and Coastal Seas around China. Journal of Atmospheric and Oceanic Technology, 27(6):1044-1058.

Liu Z, Yang H J, Liu Q, 2001. Regional dynamics of seasonal variability of sea surface height in the South China Sea. Journal of Physical Oceanography, 31(1): 272-284.

Morrow R, Traon P-Y L, 2012. Recent advances in observing mesoscale ocean dynamics with satellite altimetry. Advances in Space Research, 50, 1062-1076.

Oey L T, Ezer T, Lee H C, 2005. Loop Current, rings and related circulation in the Gulf of Mexico: a review of numerical models. In: Circulation in the Gulf of Mexico: Observations and Models. American Geophysical Union, 31-56.

Oke P R, Allen J S, Miller R N, Egbert G D, Kosro P M, 2002. Assimilation of surface velocity data into a primitive equation coastal ocean model. Journal of Geophysical Research Oceans, 107(C9): 5-1-5-25.

Oke P R, Brassington G B, Griffin D A, Schiller A, 2010. Ocean data assimilation: a case for ensemble optimal interpolation. Australian Meteorological and Oceanographic Journal, 59: 67-76.

Reynolds R W, Smith T M, Liu Chunying, et al., 2007. Daily High Resolution Blended Analyses for Sea Surface Temperature. Journal of Climate, 20(22): 5473-5496.

Rio M. H., S. Mulet, and N. Picot, 2014: Beyond GOCE for the ocean circulation estimate: Synergetic use of altimetry, gravimetry, and in situ data provides new insight into geostrophic and Ekman currents. Geophysical Research Letters, 41(24): 8918-8925.

Treguier A M, Chassignet E P, Boyer A L, Pinardi N, 2017. Modeling and forecasting the "weather of the ocean" at the mesoscale. Journal of Marine Research, 75(3): 301-329.

Uppala S, Kallberg P, Simmons A J, et al., 2005. The EAR-40 re-analysis. Quarterly Journal of the Royal Meteorological Society, 131(612): 2961-3012.

Vos M D, Backeberg B, Counillon F, 2018. Using an eddy-tracking algorithm to understand the impact of assimilating altimetry data on the eddy characteristics of the Agulhas system. Ocean Dynamics, 1-21.

Wang D X, Zhou F Z, Qin Z H, 1996. Numerical simulation of the upper ocean circulation with two-layer model. Acta Oceanologica Sinica, 18(5): 30-40.

Wang D, Xu H, Lin J, et al., 2008. Anticyclonic eddies in the northeastern South China Sea

during winter 2003/2004. Journal of Oceanography, 64: 925-935, doi: 910.1007/s10872-10008-10076-10873.

Wang G, Su J, Chu P C, 2003. Mesoscale eddies in the South China Sea observed with altimeter data. Geophysical Research Letters, 30(21): 2121, doi: 10.1029/2003GL018532.

Wang Z, Li Q, Sun L, Li S, Yang Y J, Liu S-S, 2015. The most typical shape of oceanic mesoscale eddies from global satellite sea level observations, Frontiers of Earth Science, 9 (2): 202-208. DOI 10.1007/s11707-014-0478-z.

Woodham R H, Alves O, Brassington G B, Robertson R, Kiss A, 2015. Evaluation of ocean forecast performance for Royal Australian Navy exercise areas in the Tasman Sea, Journal of Operational Oceanography, 8(2): 147-161.

Woodruff S D,Slutz R J, Jenne R L, Steurer P M, 1987. A comprehensive ocean-atmosphere data set. Bulletin of the American Meteorological Society,68(10):1239-1250.

Wu C R, Chiang T L, 2007. Mesoscale eddies in the northern South China Sea. Deep-Sea Research, Part II, 54(14): 1575-1588.

Xiao X J, Wang D X, Xu J-J, 2006. The assimilation experiment in the southwestern South China Sea in summer 2000. Chinese Science Bulletin, 51(s2): 31-37.

Xie J P, Bertino L, Cardellach E, Semmling M, Wickert J, 2018. An OSSE evaluation of the GNSS-R altimetery data for the GEROS-ISS mission as a complement to the existing observational networks, Remote Sensing of Environment, 209: 152-165.

Xie J P, Counillon F, Zhu J, Bertino L, 2011. An eddy resolving tidal-driven model of the South China Sea assimilating along-track SLA data using the EnOI. Ocean Science, 8(2): 609-627.

Xu D Z, Li X C, Zhu J, Qi Y Q, 2011. Evaluation of an ocean data assimilation system in the marginal seas around China, with a focus on the South China Sea. Chinese Journal of Oceanology and Limnology, 29(2): 414-426.

Xu D Z, Zhu J, Qi Y Q, et al., 2012. Impact of mean dynamic topography on SLA assimilation in an eddy-resolving model. Acta Oceanologica Sinica, 31(5): 11-25.

Yan C X, Zhu J, Zhou G Q, 2007. Impacts of XBT, TAO, altimetry and ARGO observations on the tropic Pacific Ocean data assimilation. Advances in Atmospheric Sciences, 24(3): 383-398.

Yang K, Shi P, Wang D X, et al., 2000. Numerical study about the mesoscale multi-eddy system in the northern South China Sea in winter. Acta Oceanologica Sinica, 22(1): 27-34.

Zhu J, 2011. Overview of Regional and Coastal Systems, Chapter 17 in Operational Oceanography in the 21st Century. Edited by A. Schiller and G. B. Brassington, PP. 727, Springer Science, Business Media B.V.

Zhuang W, Du Y, Wang D X, Xie Q, 2010: Pathways of mesoscale variability in the South China Sea. Chinese Journal of Oceanology and Limnology, 28(5): 1055-1067.

Figures:

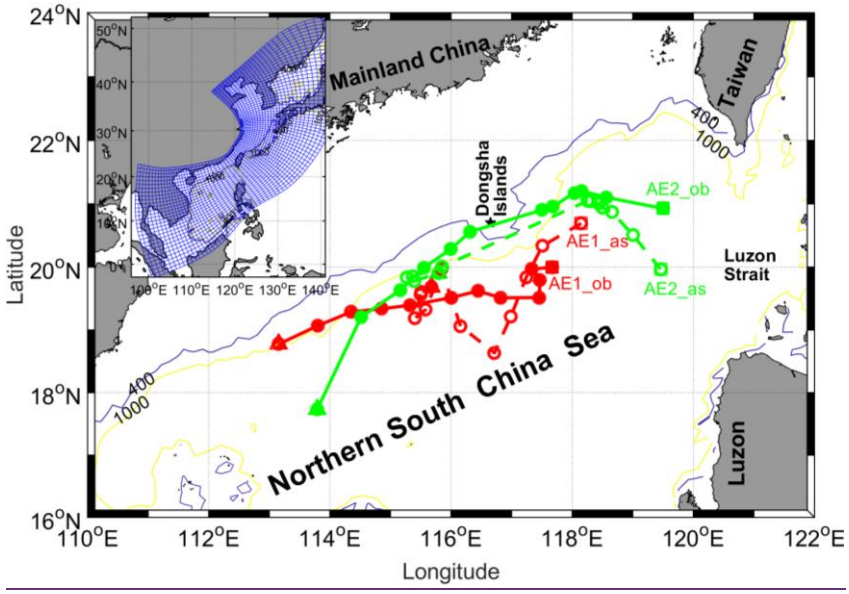

Fig. 1 Bathymetry of the northern South China Sea. The blue and yellow contour lines are the isolines of 400 m and 1000 m. The solid black Pentagram indicated Dongsha Islands. The migration path of AE1 and AE2 in the NSCS during December 2003~April 2004. Red solid (hollow) circle dots and solid (dash) lines indicated weekly passing position and migration path of observation (assimilation) AE1. Green solid (hollow) circle dots and solid (dash) lines indicated weekly passing position and migration path of observation (assimilation) AE2. The quadrangle and triangle denoted start and end position, respectively. The model domain of CSCSS (the inset panel), the curvilinear orthogonal model grid with 1/8-1/12° horizontal resolution (147×430) is denoted by the blue grid (at intervals of 10 grid cells here).

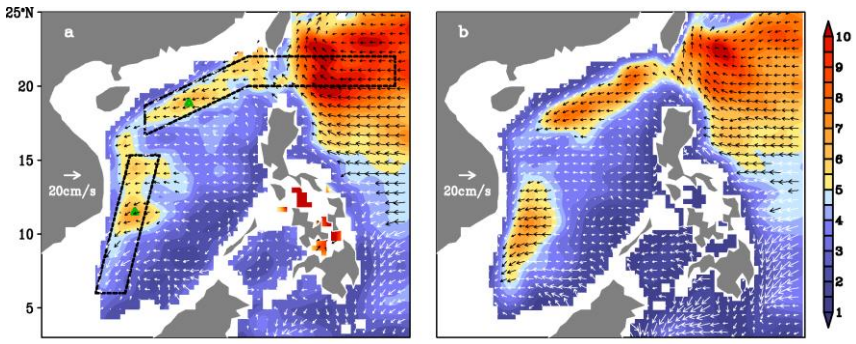

Fig. 2 Annual mean standard deviation of sea level mesoscale signals (color shading, unit: cm) and propagation velocities of the signals (vectors) derived from (a) altimeter observations; (b) OFES simulations. From Zhuang et al. (2010).

带格式的：两端对齐，行距：多倍行距 1.15 字行

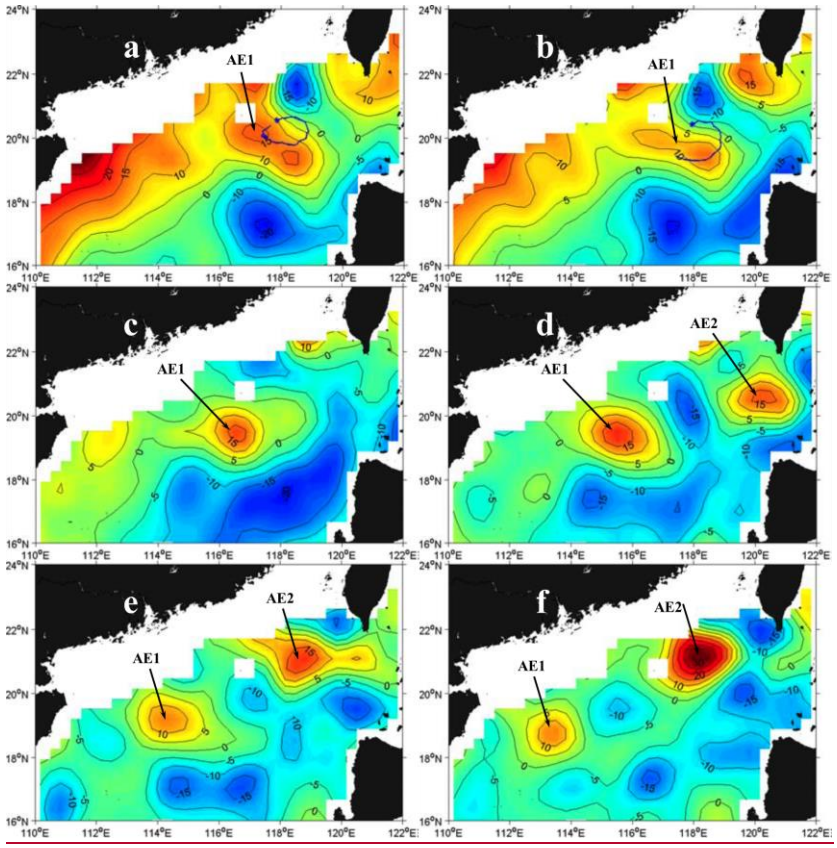

Fig. 3 –Snapshots of SLA from satellite remote sensing datasets. Buoy 22918 trajectory (blue lines, blue asterisk represents the initial position of buoy, as in Fig. 4) (a) from December 4–15, 2003 superposed on SLA field on December 10, 2003; (b) from December 16–23, 2003 superposed on SLA field on December 17, 2003; SLA field on (c) January 7, 2004; (d) January 21, 2004; (e) February 4, 2004; (f) February 18, 2004. From Wang et al. (2008).

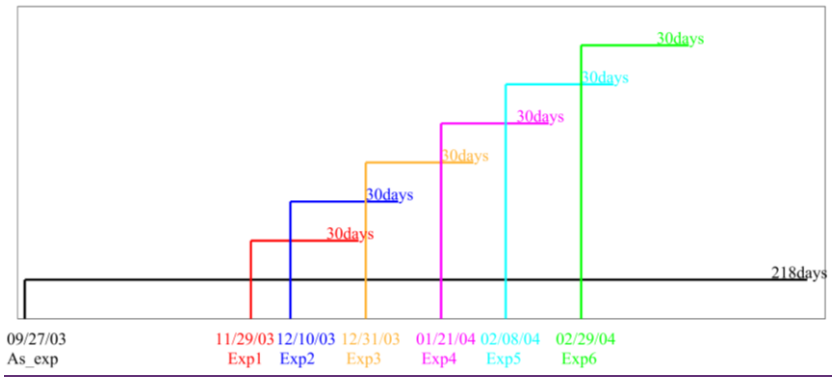

Fig. 4 The settings of assimilation and six forecast experiments, including the start and end date.

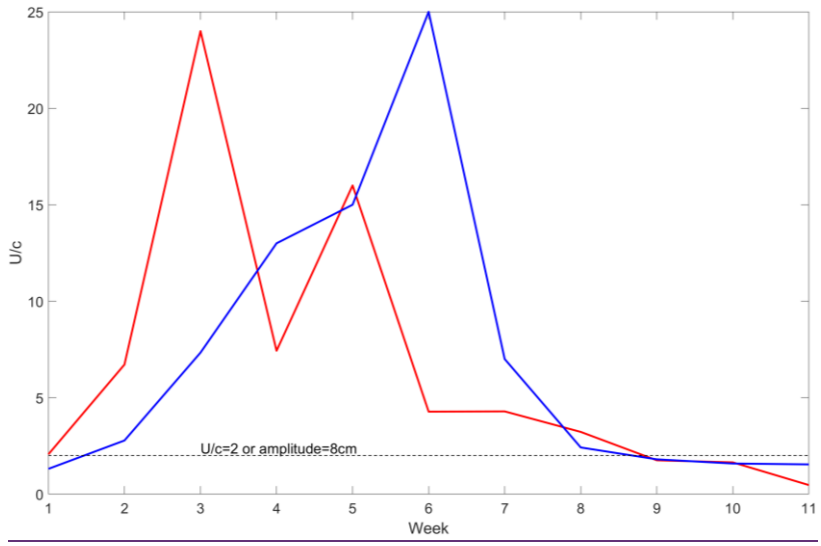

Fig. 5 The advective nonlinearity parameter U/c (ANP). The thick red (blue) curve indicates the ANP of the observed (As_exp experiment) of AE2, the dash line indicates the value of eddy amplitude at 8 cm or the ~~U/c=2~~ANP greater than 2.

带格式的：字体：Times New Roman，五号
带格式的：行距：多倍行距 1.15 字行
带格式的：字体：五号
带格式的：字体：Times New Roman，五号
带格式的：字体：五号
带格式的：字体：Times New Roman，五号
带格式的：两端对齐，行距：多倍行距 1.15 字行

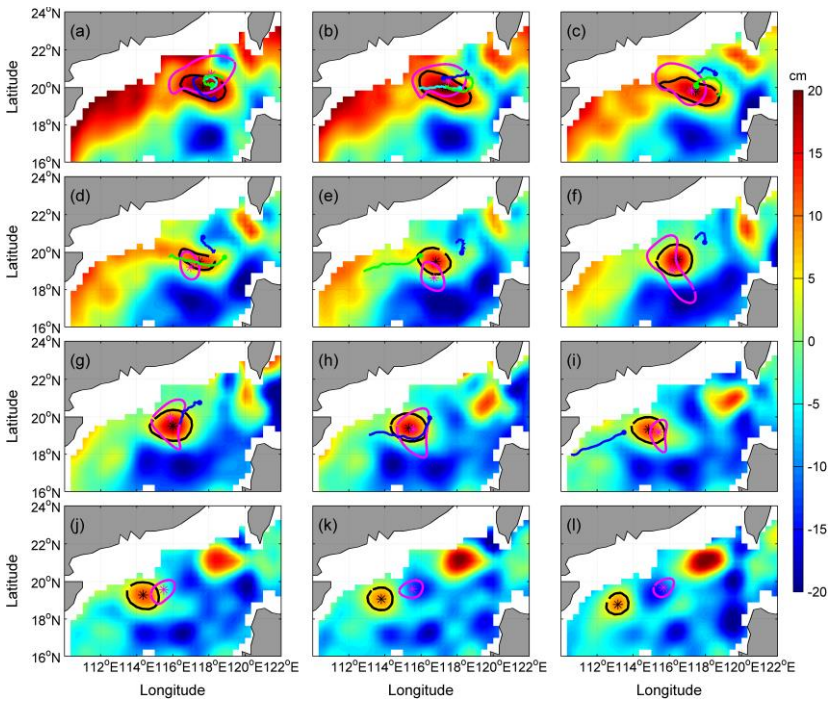

Fig. 46 Comparisons of AE1 derived from weekly SLA of assimilation results and observation from satellite remote sensing during the period of December 2003~February 2004. Background color is SLA, "*" mark and closed lines indicated the center position and the outermost closed isoline of AE1, respectively, the black is from satellite observation SLA, the pink is from assimilation SLA. The cyan, green and blue solid circle lines indicated the start positions and trajectories of number 22517, 22918 and 22610 drifter buoys, respectively. (a)-(l) is SLA on the 3rd of December 2003~ the 18th of February 2004, respectively. Unit: cm.

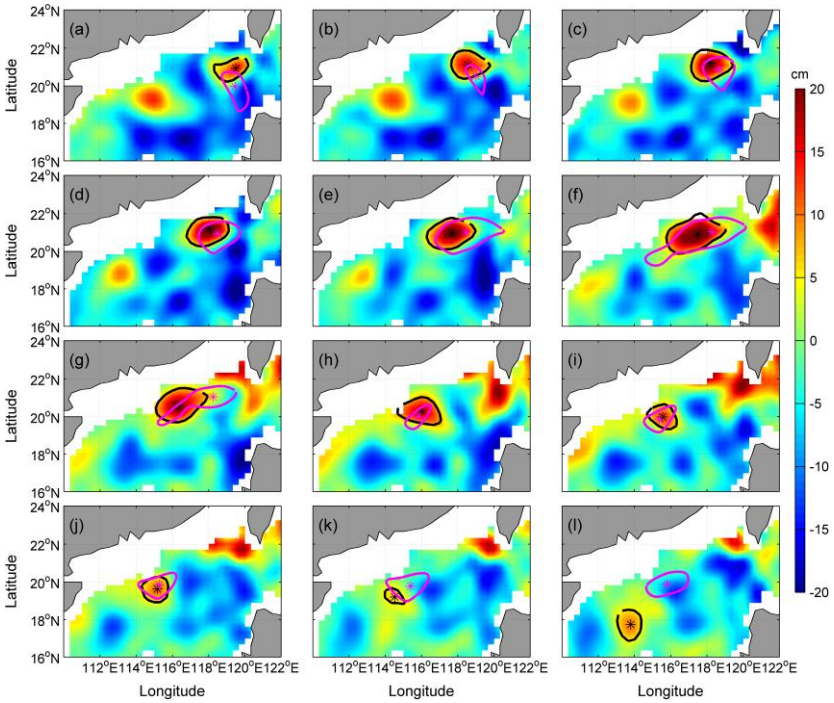

Fig. ~~5~~7 The same as figure 4, But for AE2, the corresponding period is January 28th, 2003~April 14th, 20

Tables：

Table 1 The amplitude of AE1 and AE2 derived from observation SLA and the assimilation SLA, and distance of eddy centers between the observation SLA's and assimilation SLA's.

Weekly			1(2003/12/3)	2	3	4	5	6	7	8	9	10	11	12
AE1	Distance (km)		94	45	26	62	98	70	54	30	63	131	199	298
	Amplitude(cm)	Observed	8	10	9	8	8	13	13	11	8	8	4	6
		Assimilated	18	12	11	6	5	4	5	6	2	3	3	2
Weekly			1(2004/1/28)	2	3	4	5	6	7	8	9	10	11	12
AE2	Distance (km)		107	83	67	57	85	91	221	36	26	26	117	328
	Amplitude(cm)	Observed	7	12	18	17	17	16	15	10	7	6	N/A	6
		Assimilated	3	2	5	6	10	8	4	8	9	4	5	6

带格式的：编号方式：连续

Table 2 The amplitude of AE1 and AE2 derived from observation SLA and the six forecast SLA, and distance of eddy centers between the observation SLA's and forecast SLA's.

Weekly				1	2	3	4	5
Exp1	Distance (km)			80	58	32	68	47
	Amplitude (cm)		Observed	8	10	9	8	8
			Forecasted	14	12	14	11	12
Exp2	Distance (km)			57	22	63	51	113
	Amplitude (cm)		Observed	10	9	8	8	13
			Forecasted	12	11	6	8	10
Exp3	Distance (km)			134	85	111	130	124
	Amplitude (cm)		Observed	13	13	11	8	8
			Forecasted	2	3	3	3	N/A
Exp4	AE1	Distance (km)		32	58	111	161	231
		Amplitude (cm)	Observed	11	8	8	4	6
			Forecasted	4	2	2	2	N/A
	AE2	Distance (km)		N/A	N/A	132	95	81
		Amplitude (cm)	Observed	N/A	N/A	12	18	17
			Forecasted	N/A	N/A	N/A	6	9
Exp5	AE1	Distance (km)		188	274	287	405	503
		Amplitude (cm)	Observed	4	6	2	N/A	N/A
			Forecasted	2	2	2	2	2
	AE2	Distance (km)		69	77	102	95	226
		Amplitude (cm)	Observed	18	17	17	16	15
			Forecasted	5	7	6	6	9
Exp6	AE2	Distance (km)		91	227	277	339	453
		Amplitude (cm)	Observed	16	15	10	7	6
			Forecasted	7	9	6	4	6

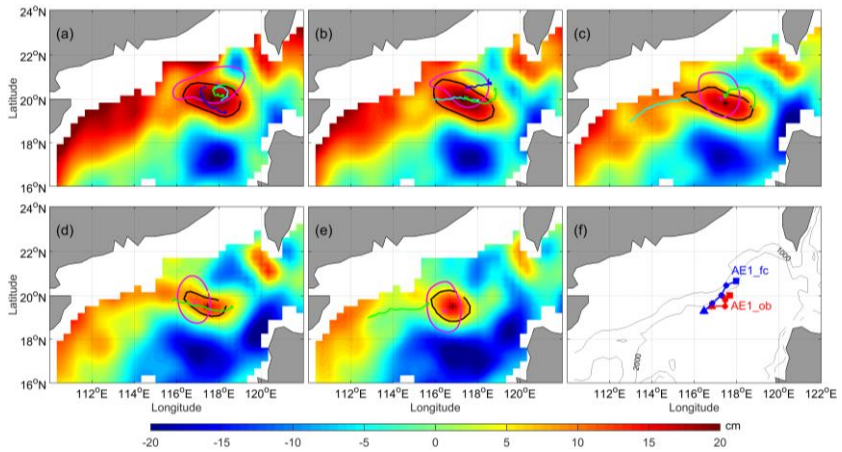

Fig. ~~6~~8 Comparison of AE1 of Exp1 and observation, and trajectories of drifter buoys during the 29th of November 2003 and the 29th of December 2004. The cyan, green and blue solid circle dots and lines indicated the start positions and trajectories of number 22917, 22918 and 22610 drift buoys during the corresponding period, respectively. Where, the red (blue) dotted line in (f) is the moving path of AE1 derived from observation (forecast) SLA during the experiment period, the square (triangle) represents the start (end) position.

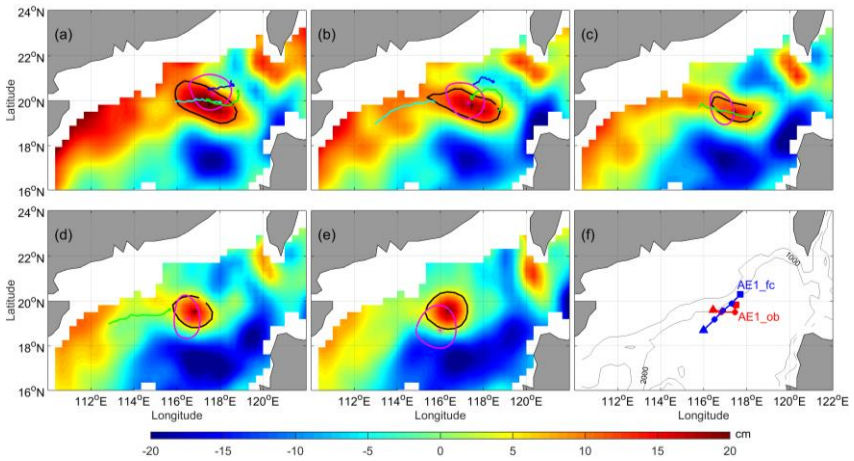

Fig. ~~7~~9 Same as figure ~~6~~8, but for Exp2, the experiment period is the 10th of December 2003 to the 9th of January 2004.

带格式的：编号方式：连续

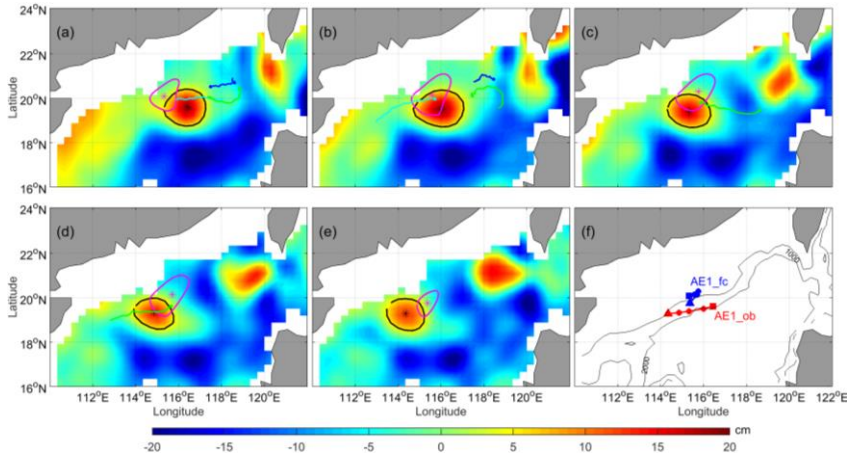

Fig. ~~8~~10 Same as figure ~~7~~9, but for Exp3, the experiment period is the 31st of December 2003 to the 30th of January 2004.

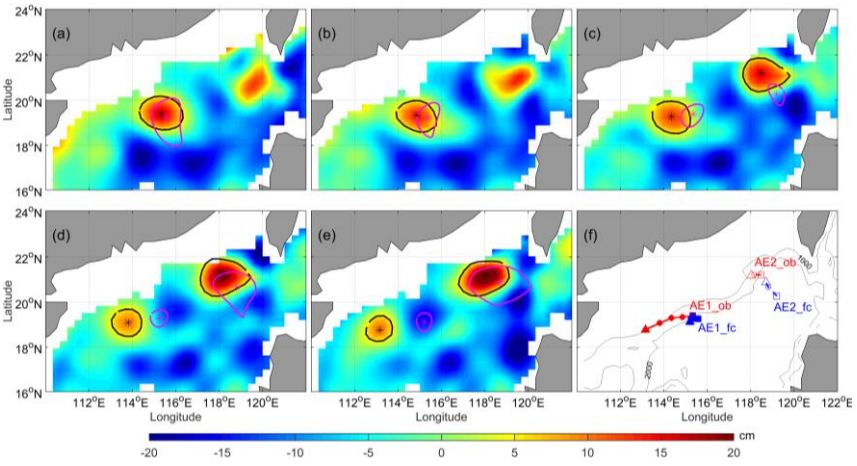

Fig. ~~9~~11 Same as figure 8, but for Exp4，where, the red (blue) dotted line in (f) is the observation (forecast) moving path of AE1 and AE2. the red solid (dashed) lines and solid (hollow) circle derived from observation SLA for AE1 (AE2), the blue solid (dashed) lines and solid (hollow) circle derived from forecast SLA during the 21st of January 2004 to the 20th of February 2004.

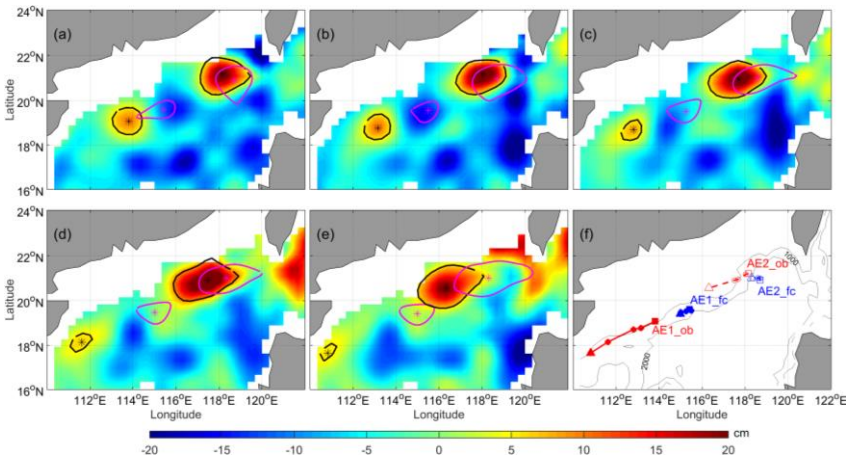

Fig. 102 Same as figure 911, but for Exp5, the experiment period is the 8th of February 2004 to the 10th of March 2004.

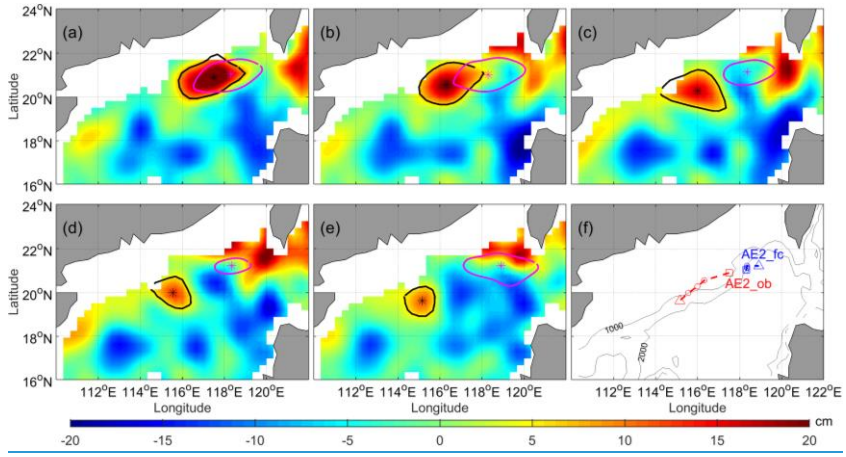

Fig. 113 Same as figure 911, but for Exp6 and AE2, the experiment period is the 29th of February 2004 to the 30th of March 2004.

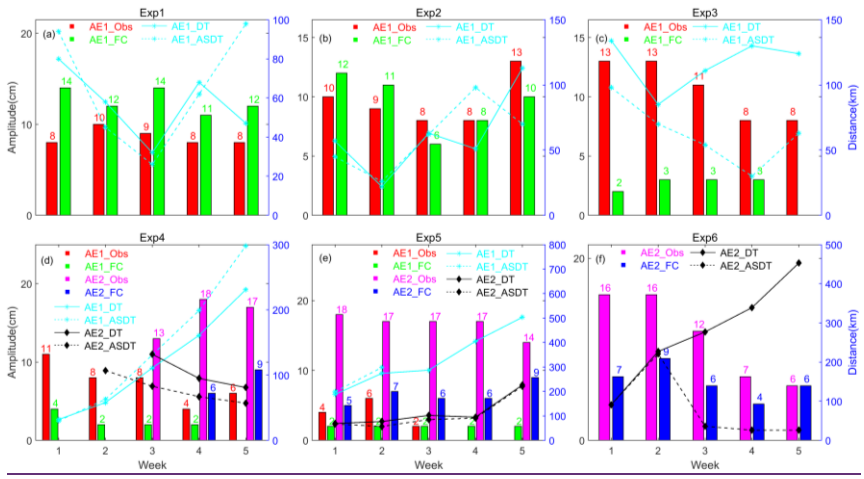

Fig. 14 The amplitude of AE1 and AE2 derived from observation SLA and the six forecast SLA, and distance of eddy centers between the observation, assimilation and forecast SLA's, respectively. The red and green histograms indicated the AE1 amplitudes from observation and prediction respectively. The pink and blue histograms expressed the AE2 amplitudes from observation and prediction respectively. The cyan star solid (dash) line shows the distance of the center between observation and prediction (assimilation) AE1. The black diamond solid (dash) line shows the distance of the center between observation and prediction (assimilation) AE2.

带格式的：行距：多倍行距 1.15 字行